



The use of Feynman diagrammatic approach for well test analysis in stochastic porous media

A. V. Novikov¹ · D. V. Posvyanskii²

Received: 1 November 2018 / Accepted: 20 August 2019 / Published online: 10 September 2019
© Springer Nature Switzerland AG 2019

Abstract

Transient well test analysis provides valuable information about reservoir characteristics such as permeability and the hydraulic diffusivity coefficient. It is based on the solution of diffusivity equation, which describes mass transfer in porous media. On the whole, analytical solutions are used for interpreting well test data. However, all these solutions were obtained under the condition of reservoir homogeneity. In a heterogeneous reservoir with spatially variable permeability, the exact analytical solutions are not known. The heterogeneous permeability field can be represented as the sum of two terms. The first term is a constant mean permeability value and the second one is a random function with known statistical properties. The second term can be considered a perturbation. The possibility of evaluating geostatistical parameters from well test analysis was considered by various authors and is still a challenging problem. In a randomly heterogeneous reservoir, a flow equation is formulated for the pressure, which is averaged over all the permeability realizations. It can be solved using Green's function techniques, where the ensemble-averaged pressure is represented as an infinite perturbation series. This series can be represented graphically using Feynman diagrams and its summation can be performed following the rules that are well known in the quantum theory of solid state. For the first time, this framework was introduced to reservoir simulation in King (J. Phys. A: Math. Gen. **20**, 3935–3947, 1987), where the stochastic pressure equation was solved for the steady-state case. In this study, we use diagram approach to obtain the solution of the time-dependent stochastic pressure equation which is derived for a lognormal random permeability field under the assumption of the Gaussian correlation function. The expression for transient ensemble averaged pressure is obtained with respect to high-order corrections of permeability variance. In the limit of sufficiently small variance, analytical expressions for the pressure correction are presented. The two limiting cases were considered: (i) the distance between wells is much bigger than the permeability correlation length; (ii) the opposite case where the correlation length is the smallest length parameter. The resulting solution can be used for the analysis of drawdown, build-up, and interference tests in stochastic porous media. The possibility of estimating the parameters of a random permeability field based on well test data is discussed.

Keywords Green's function · Well test · Stochastic media · Feynman diagrams

Mathematics Subject Classification (2010) 35J05 · 40H05

1 Introduction

Permeability has a significant effect on fluid flow in a porous media. Effective reservoir development can be carried out if the permeability field is well-known. However,

it is known only at some spatial points where wells are located and there is practically no information about the values between them. The permeability distribution can be approximated using different interpolation methods; however, this approach does not provide a unique solution. It leads to uncertainties in reservoir properties, and as a result, uncertainties in the prediction of production data. On the other hand, well test analysis provides important information about the interwell permeability distribution of a reservoir. The standard methods for its analysis are based on the assumption that the reservoir is uniform and

✉ D. V. Posvyanskii
Dimitrii.Posvyanskii@Emerson.com

Extended author information available on the last page of the article.

its permeability is a constant. The solution of the diffusivity equation for a homogeneous reservoir is well-known

$$\Delta p = -\frac{q\mu}{4\pi kh} Ei\left(-\frac{r^2}{4\kappa t}\right), \quad (1)$$

where diffusivity $\kappa = k/\mu mc_t$, k is scalar permeability, m is porosity, c_t is compressibility, μ is fluid viscosity, h is the reservoir thickness, and q denotes fluid flow rate. This expression is widely used in well test analysis. It allows reservoir properties to be estimated from the measurement of wellbore pressure and production rate over time. However, reservoir permeability varies in space and the use of the standard approach for homogeneous media leads to errors in the estimation of reservoir parameters. Therefore, the problem of well inflow modeling in heterogeneous reservoir becomes important.

Fluid flow in a random porous medium was considered in a number of papers. One of the possible approaches is to generate a number of stochastic permeability realizations and to calculate pressure distribution for each one using the reservoir simulator. The pressure realizations obtained should also be averaged. Such an approach is usually called a Monte-Carlo simulation (MCS), which is widely used in geological and flow simulation. However, this method is rather time consuming. The other framework is a perturbation-based stochastic flow simulation that employs probabilistic approach of governed balance equations with respect to statistical moments.

The problem was formulated as finding the solution of a flow equation where permeability was treated as a random field. In other words, it is a partial differential equation with stochastic coefficient and its solution is the pressure averaged over the ensemble of all spatial permeability realizations. To our knowledge, one of the first studies of this problem was presented in [1]. This work was concerned with the problem of averaging the flow in stochastic porous media. The heterogeneity of the porous media was considered as a perturbation and the solution of the equation with stochastic coefficient was expanded in a series of the powers of perturbation. However, this expansion was terminated at the second order, so it was supposed that the permeability distribution had a small variance compared with the mean permeability.

In [2], Feynman diagram technique was proposed to solve the steady state flow equation in randomly heterogeneous media. From the formal point of view, the problem was reduced to finding Green's function of Laplace equation averaged over all permeability realizations. In contrast to the perturbation method, this technique allows for the most significant terms in the infinite perturbation series to be calculated. Using this approach, the ensemble-averaged pressure, its variance, and the effective permeability of porous media can be calculated. One of the conclusions of

[2] was that the effective permeability does not depend on the correlation length of a random permeability.

Numerical investigations of liquid flow in stochastic porous media were carried out in [3, 4]. Perturbation theory allows equations with respect to several perturbative terms to be derived for the first two statistical moments. The steady-state single-phase flow in a bounded nonuniform geological reservoir was considered in [3] and the effects of statistical non-stationarity and the presence of boundaries were investigated. The case of two-phase transient flow in random porous media was studied at [5].

Transient flow in random heterogeneous media was studied in [6, 7] where the effective reservoir permeability was calculated analytically using second-order approximation in the standard deviation of a random permeability field. It was shown that the effective permeability is a function of time. In [8], the unsteady well inflow in a heterogeneous reservoir was considered within a diagrammatic framework, where the solution scheme, applied to Fourier-Laplace transformed equations, is similar to that used in [2]. An integral equation for ensemble averaged pressure was used for interpretation of pumping test data. It was shown that effective permeability estimated from the well test coincides with the stationary value in long time limit. However, no expressions for effective permeability were given.

All analytical solutions of diffusivity equation with random coefficient are limited to the case of a small variance of a random permeability field. Numerical well test simulation allows dealing with permeability of a wider range of the variance. MCS approach to the transient well flow in reservoir with a random permeability was presented in [9]. Single-phase flow simulations were performed for each realization of random permeability field and well test response was related to parameters of permeability distribution. However, this approach is time consuming since the results were averaged over a large number of realizations.

In this paper, we consider transient flow in stochastic porous media. Following [2], we use Feynman diagram technique to solve the diffusivity equation where permeability is treated as a random field. The resulting expression for time-dependent ensemble averaged pressure can be used to analyze well test data.

2 Mathematical model

A single-phase flow of slightly compressible fluid in a heterogeneous reservoir produced by well is described by the diffusion equation.

$$\frac{\partial p}{\partial t} = \nabla(\kappa(\mathbf{r})\nabla p) + F(\mathbf{r}, t), \quad (2)$$

where the term $F(\mathbf{r}, t)$ denotes an external source that is treated as a well. It is given by

$$F(\mathbf{r}, t) = \frac{q(\mathbf{r}, t)}{mc_t},$$

where $q(\mathbf{r}, t)$ is a distribution of source or sink points. As we mentioned above, the diffusivity coefficient is proportional to permeability $k(\mathbf{r})$. Other parameters such as the porosity, the viscosity, and compressibility are assumed to be constants. In this study, we will consider infinite reservoir produced by entire vertical well and the term $F(\mathbf{r}, t)$ is given by

$$F(\mathbf{r}, t) = \frac{q(t)\delta(\mathbf{r} - \mathbf{r}_0)}{mc_t}$$

here, \mathbf{r}_0 is coordinate of the well, and $q(t)$ defines well rate over time.

We assume that the permeability field can be decomposed into a constant mean permeability $\langle k \rangle$ and a stochastic term $\tilde{k}(\mathbf{r})$

$$k(\mathbf{r}) = \langle k \rangle + \tilde{k}(\mathbf{r}), \tag{3}$$

$\tilde{k}(\mathbf{r})$ is assumed to be stationary random field which has zero mean value. Since $\tilde{k}(\mathbf{r})$ is statistically homogeneous, the covariance function depends on the distance vector of the positions. For the same reason, the following consideration assumes unconditional permeability field.

The formal solution of (2) can be written as

$$\langle p(\mathbf{r}, t) \rangle = \int_0^t dt' \int d\mathbf{r}' \langle G(\mathbf{r}, \mathbf{r}', t') \rangle F(\mathbf{r}', t), \tag{4}$$

where $G(\mathbf{r}, \mathbf{r}', t')$ is Green’s function of (2) and $\langle \dots \rangle$ represents the ensemble averaging over different realizations of the random permeability field [10]. Formally, the problem of solving well inflow equation reduces to the estimation of $\langle G(\mathbf{r}, \mathbf{r}', t) \rangle$.

Applying Laplace transform to (2), we obtain equation for p_s

$$sp_s = \nabla(\kappa(\mathbf{r})\nabla p_s) + F_s(\mathbf{r}), \tag{5}$$

where

$$p_s(\mathbf{r}) = \mathcal{L}[p(\mathbf{r}, t)], \quad F_s(\mathbf{r}) = \mathcal{L}[F(\mathbf{r}, t)].$$

Symbol \mathcal{L} means Laplace transform.

Substituting (3) into (5) and using the definition of Green’s function, we obtain the equation with respect to the Green’s function for (5)

$$-\langle \kappa \rangle \Delta G(\mathbf{r}, \mathbf{r}') + sG(\mathbf{r}, \mathbf{r}') = \nabla(\tilde{\kappa}(\mathbf{r})\nabla G(\mathbf{r}, \mathbf{r}')) + \delta(\mathbf{r} - \mathbf{r}'). \tag{6}$$

In the case of homogeneous reservoir, (6) is the Helmholtz equation [11] and its solution is the unperturbed Green’s

function $G_0(\mathbf{r} - \mathbf{r}')$. The solution of (6) may be written as an integral equation

$$G(\mathbf{r}, \mathbf{r}') = G_0(\mathbf{r}, \mathbf{r}') + \int d\mathbf{r}_1 G_0(\mathbf{r}, \mathbf{r}_1) \nabla(\tilde{\kappa}(\mathbf{r}_1)\nabla G(\mathbf{r}_1, \mathbf{r}')). \tag{7}$$

Integral equation (7) with respect to $G(\mathbf{r}, \mathbf{r}')$ is exact (in the quantum field theory it is called as Dyson’s equation); however, its exact solution can’t be obtained easily. As usual, it can be solved iteratively. The system is assumed to be statistically homogeneous and it is more convenient to solve equation (7) in the reciprocal Fourier space. It can be rewritten in the following form

$$G(\mathbf{p}, \mathbf{q}) = 2\pi G_0(\mathbf{p})\delta(\mathbf{p} + \mathbf{q}) - G_0(\mathbf{p}) \int d\mathbf{p}'(\mathbf{p} \cdot \mathbf{p}')G(\mathbf{p}', \mathbf{q})\tilde{\kappa}(\mathbf{p} - \mathbf{p}'). \tag{8}$$

The solution of this equation can be expanded in terms of a perturbation series

$$G(\mathbf{p}, \mathbf{q}) = G_0(\mathbf{p}, \mathbf{q}) + G_1(\mathbf{p}, \mathbf{q}) + G_2(\mathbf{p}, \mathbf{q}) + \dots \tag{9}$$

To calculate well inflow in a random heterogeneous reservoir, it is necessary to calculate Green’s function averaged over all realizations of a random permeability field. For this purpose, the series (9) should be averaged term by term

$$\langle G(\mathbf{p}, \mathbf{q}) \rangle = G_0(\mathbf{p}, \mathbf{q}) + \langle G_1(\mathbf{p}, \mathbf{q}) \rangle + \langle G_2(\mathbf{p}, \mathbf{q}) \rangle + \dots \tag{10}$$

To calculate the sum (10), it is convenient to use Feynman diagrammatic representation. Diagram techniques allows to perform cumbersome calculations easily enough. Within this approach, each term in the series corresponds to a diagram which is constructed according to the certain rules, which are presented in Appendix. By inspecting the terms in the perturbation series and the corresponding diagrams, it is possible to see that some diagrams are composed of linked diagrams appearing at lower order in the expansion. Each diagram can be referred as irreducible or reducible. The diagrams which do not fall into two pieces if only one internal line is cut are referred to irreducible. The reducible diagrams can be separated into independent diagrams and two acceptable chains of nodes are generated.

The method of Feynman diagrams is widely used in quantum mechanics and many-body perturbation theory, where the sum of all irreducible diagrams is called “self-energy” and below we use this terminology. The derivation of ensemble averaged Green’s function is presented in Appendix. The expression for $\langle G(\mathbf{p}) \rangle$ can be written in a rather compact form

$$\langle G(\mathbf{p}) \rangle = \frac{G_0(\mathbf{p})}{1 - G_0(\mathbf{p})\Sigma(\mathbf{p})}, \tag{11}$$

where Σ denotes the self-energy. It is given by the expression

$$\Sigma(\mathbf{p}) = G_0(\mathbf{p}) \int d\mathbf{p}' G_0(\mathbf{p}') (\mathbf{p} \cdot \mathbf{p}') (\mathbf{p}' \cdot \mathbf{p}) C(\mathbf{p} - \mathbf{p}'), \quad (12)$$

where $C(\mathbf{p} - \mathbf{p}')$ is Fourier transform of the covariance function of the permeability random field. As can be seen from (11), it is nothing but a sum of the geometric progression and the self-energy is its common ratio. It is well-known that the progression converges if the common ratio is less than one. This corresponds the situation when permeability standard deviation is approximately equal to mean permeability. This condition restricts the usage of Feynman diagram approach.

An effective permeability of heterogeneous porous media k^* can be expressed through the self-energy [2]

$$k^* = \langle k \rangle - \frac{\Sigma(\mathbf{p})}{\mathbf{p}^2} \quad (13)$$

Once we have calculated the ensemble averaged Green's function, it should be substituted in (4) and the mean pressure can be calculated. Below, we will consider the use of this expression for mean pressure to interpret transient well tests.

3 Transient pressure behavior in heterogeneous reservoir

In this section, we apply diagrammatic technique to calculate transient pressure behavior in a heterogeneous infinite 2D reservoir produced by a vertical well. For this task, the bare Green's function is

$$G_0(\mathbf{r} - \mathbf{r}') = \frac{1}{2\pi} K_0 \left(\sqrt{\frac{s}{\langle \kappa \rangle}} |\mathbf{r} - \mathbf{r}'| \right), \quad (14)$$

where K_0 is modified Bessel function of the second kind. Applying Fourier transform,

$$G_0(\mathbf{p}) = \frac{1}{2\pi \langle \kappa \rangle} \frac{1}{\mathbf{p}^2 + s/\langle \kappa \rangle}. \quad (15)$$

For lognormal permeability distribution, the covariance function can be written as

$$C(\mathbf{r} - \mathbf{r}') = \langle \kappa \rangle^2 \left(e^{\sigma_y^2 \rho_y(\mathbf{r} - \mathbf{r}')} - 1 \right), \quad (16)$$

where σ_y^2 and $\rho_y(\mathbf{r} - \mathbf{r}')$ are variance and correlation functions of $y(\mathbf{r}) = \ln k(\mathbf{r})$, see in [12]. The typical correlation function is exponentially decaying over the correlation length λ

$$\rho_y(\mathbf{r} - \mathbf{r}') = e^{-|\mathbf{r} - \mathbf{r}'|^2/\lambda^2} \quad (17)$$

The covariance (16) can be presented as an expansion with respect to powers of σ_y^2 and for $\sigma_y^2 < 1$

$$C(\mathbf{r} - \mathbf{r}') \approx \langle \kappa \rangle^2 \sigma_y^2 \rho_y(\mathbf{r} - \mathbf{r}') + o(\sigma_y^4)$$

Substituting (15) and (17) into (12) yields expression for the self-energy. Then applying the inverse Laplace transform, we obtain the expression for the mean pressure

$$\langle p(\mathbf{r}, t) \rangle = \frac{\mu}{2\pi kh} \int_0^\infty d\eta \eta J_0 \left(\eta \frac{\Delta r}{\lambda} \right) \times \mathcal{L}^{-1} \left[\frac{q_s}{\left(\eta^2 \Phi(\sigma_y^2, \eta) + s\lambda^2/\kappa \right)} \right], \quad (18)$$

where $\Phi(\sigma_y^2, \eta) = [1 - \sigma_y^2 f(\eta)]$ and \mathcal{L}^{-1} means inverse Laplace transform.

The function $f(\eta)$ is defined by the expression

$$f(\eta) = \int_0^\infty d\xi \xi e^{-(\eta^2 + \xi^2)/4} \left(\frac{I_1(\eta\xi/2)}{\eta\xi/2} - I_2(\eta\xi/2) \right)$$

where I_n is the modified Bessel function of the first kind. In general, this function can be computed numerically. However, in two extreme cases of small and large values of η

$$f(\eta) = \begin{cases} 1/2, & \eta \ll 1 \\ 1.0, & \eta \gg 1 \end{cases}$$

It should be noted that in (18) nothing was assumed about well rate time dependence. This expression can be used for well test analysis in stochastic reservoirs. There are various types of well tests such as pressure build up, drawdown, and interference test. Below, we will demonstrate how to use (18) for well test interpretation.

Drawdown test In this test, the well is produced at the constant rate for a period of time. Bottom hole pressure declines during the test and reservoir parameters can be estimated with the analysis of a transient pressure behavior. The well is expected to be produced at constant rate; however, in practice, the wellbore storage effect exists and q_s is given by

$$q_s = \frac{q_0}{s^2\tau + s},$$

where q_0 is a target rate and τ is a characteristic time of the wellbore storage effect. Δr is equal to wellbore radius r_w and $r_w \ll \lambda$.

The mean pressure is given by the expression

$$\langle p(\mathbf{r}, t) \rangle = p_D \int_0^\infty \frac{d\eta J_0\left(\eta \frac{\Delta r}{\lambda}\right)}{\eta \Phi(\sigma_y^2, \eta)} \times \left(1 + \frac{e^{-\eta^2 \Phi(\sigma_y^2, \eta) \frac{t}{t_D}} - \eta^2 \Phi(\sigma_y^2, \eta) \frac{\tau}{t_D} e^{-t/\tau}}{\eta^2 \Phi(\sigma_y^2, \eta) \frac{\tau}{t_D} - 1} \right), \tag{19}$$

where $p_D = q_0 \mu / 2\pi \langle k \rangle h$, $t_D = \lambda^2 / \kappa$.

The difficulty of calculating the integral (19) is related to the fact that it consists of two divergent at $\eta = 0$ terms; however, the whole integral is regular. Taking derivative eliminates this difficulty

$$\frac{\partial \langle p \rangle}{\partial \ln t} = -p_D \frac{t}{t_D} \int_0^\infty d\eta \eta J_0\left(\eta \frac{\Delta r}{\lambda}\right) \times \left(\frac{e^{-\eta^2 \Phi(\sigma_y^2, \eta) t/t_D} - e^{-t/\tau}}{\eta^2 \Phi(\sigma_y^2, \eta) \frac{\tau}{t_D} - 1} \right) \tag{20}$$

Figure 1 shows time dependencies of the dimensionless pressure logarithmic derivative calculated for different values of a correlation length. All curves demonstrate wellbore storage period as well as two periods where

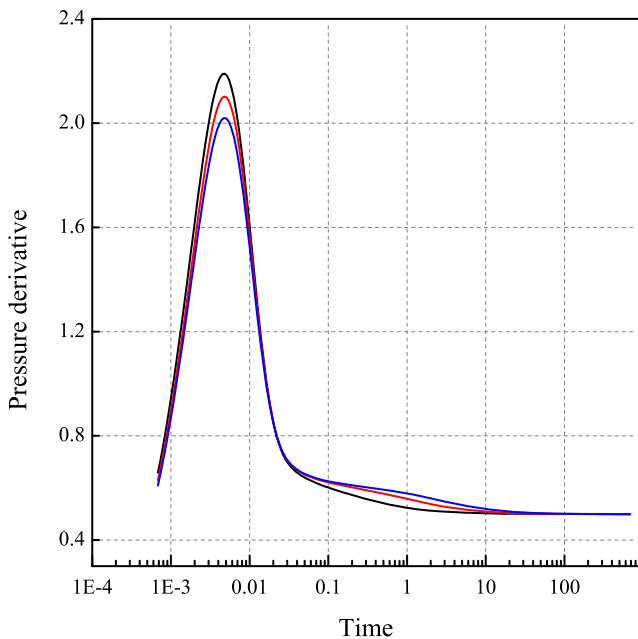


Fig. 1 Dimensionless logarithmic pressure derivatives for different values of correlation length and $\sigma_y^2 = 0.3$. Derivatives are normalized to geometric mean permeability whereas time is normalized to scale $\lambda^2 / \langle \kappa \rangle$ with $\lambda = 100$ m. The black, red, and blue curves correspond to $\lambda = 100$ m, $\lambda = 200$ m, and $\lambda = 300$ m respectively. The dimensionless time of wellbore storage effect is equal to 4×10^{-3}

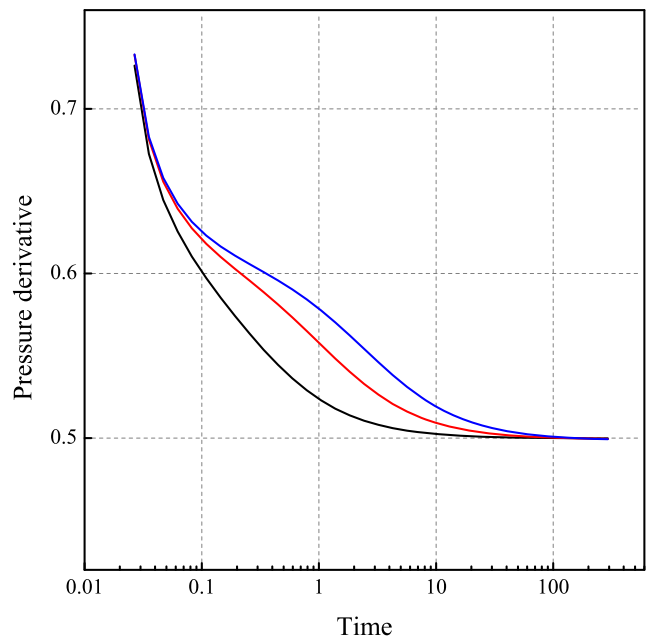


Fig. 2 Transition region between two stabilization periods of pressure derivatives for different values of correlation length and $\sigma_y^2 = 0.3$. Derivatives are normalized to geometric mean permeability whereas time is normalized to scale $\lambda^2 / \langle \kappa \rangle$ with $\lambda = 100$ m. The black, red, and blue curves correspond to $\lambda = 100$ m, $\lambda = 200$ m, and $\lambda = 300$ m respectively

the pressure derivative is stabilized. The first stabilization period is observed at early times

$$\frac{t}{t_D} < 1$$

and corresponds to the harmonic mean permeability k_H . The second plateau is observed at the late time when the investigation radius is beyond the correlation length. It corresponds to the geometric mean permeability k_G . Between two stabilization periods, there is transition region where the pressure derivative changes rapidly. Transition region is observed at times $t_D \sim \lambda^2 / \langle \kappa \rangle$ and it is shown in Fig. 2. The wellbore storage effect reduces initial plateau. At long times, all curves have the same value. It means that the effective reservoir permeability does not depend on correlation length. It corresponds to the conclusions of [1, 2].

Increase of the effective reservoir permeability with time depends on the variance of the random permeability field. Figure 3 illustrates time dependencies of pressure derivative calculated for different values of σ_y^2 .

It is convenient to present mean pressure as the sum of two terms

$$\langle p(\mathbf{r}, t) \rangle = p_0(\mathbf{r}, t) + \langle \delta p(\mathbf{r}, t) \rangle,$$

where the first term p_0 denotes pressure distribution in a homogeneous reservoir, and $\langle \delta p(\mathbf{r}, t) \rangle$ is the correction due to medium heterogeneity. It depends on the variance of the random permeability field.

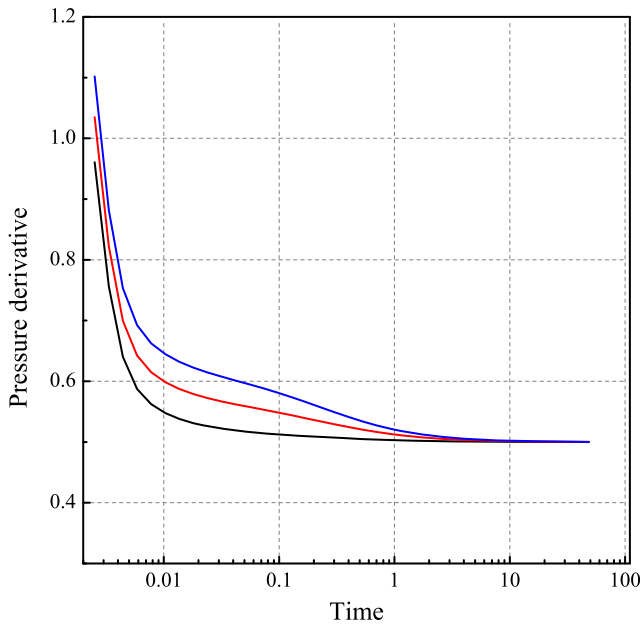


Fig. 3 Dimensionless logarithmic pressure derivatives for different values of permeability variance and $\lambda = 100$ m. Derivatives are normalized to geometric mean permeability whereas time is normalized to scale $\lambda^2/\langle k \rangle$ with $\lambda = 100$ m and $\sigma_y^2 = 0.05$. The black, red, and blue curves correspond to $\sigma_y^2 = 0.05, \sigma_y^2 = 0.2$, and $\sigma_y^2 = 0.3$ respectively

If $\sigma_y^2 \ll 1$, the perturbation series can be terminated at the second order with respect to standard deviation σ_y . For a long time limit $t/t_D \gg 1$, the analytical expression for $\langle p(\mathbf{r}, t) \rangle$ can be written as

$$\langle \delta p(\mathbf{r}, t) \rangle = -\sigma_y^2 \frac{pD}{4} \ln \left(\frac{\lambda^2}{4\bar{k}t} \right) \quad (21)$$

Generally, the effective permeability of reservoir can be written as

$$k^*(t) = \langle k \rangle \left(1 - g(\sigma_y^2, t) \right), \quad (22)$$

where $g(\sigma_y^2, t)$ is dimensionless correction due to the permeability fluctuation. If $\sigma_y^2 \ll 1$ and $t/t_D \gg 1$, the expression for k^* is given by

$$k^* = \langle k \rangle \left(1 - \frac{\sigma_y^2}{2} \right) \approx \langle k \rangle e^{-\sigma_y^2/2} = k_G. \quad (23)$$

Expression (24) represents a second-order perturbation expansion of $\langle p(\mathbf{r}, t) \rangle$ and the limit of its applicability is $\sigma_y^2 \ll 1$. Expression (24) coincides with the steady-state effective permeability given in [1, 2, 13].

For $t/t_D \ll 1$ and $\sigma_y^2 \ll 1$ then

$$k^* = \langle k \rangle \left(1 - \sigma_y^2 \right) = k_H. \quad (24)$$

This expression was obtained in [1]; however, the perturbation series was terminated at second order.

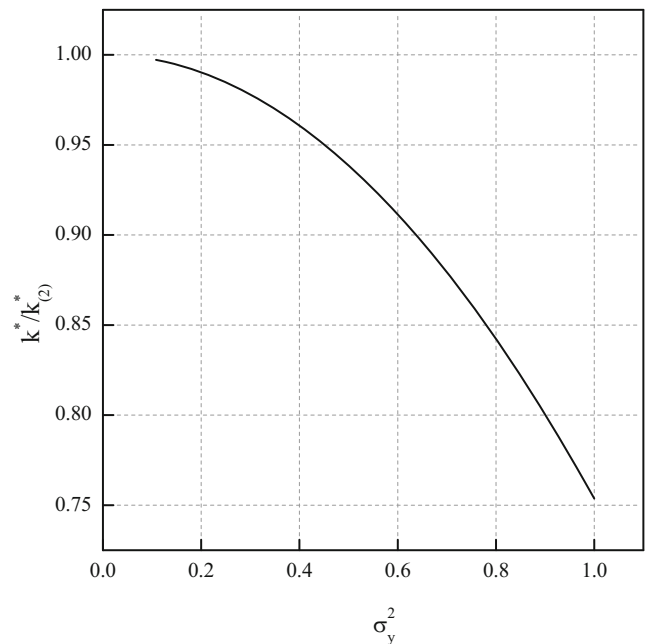


Fig. 4 Effective permeability ratio againsts the variance of the gaussian random permeability field

As it was mentioned above, Feynman diagrammatic approach allows going beyond the linear approximation in σ_y^2 and to calculate higher-order corrections to the effective permeability.

Figure 4 shows the dependence of the effective permeability ratio on the variance σ_y^2 in the case of Gaussian random permeability field. The permeability ratio is defined as $k^*/k_{(2)}^*$, where $k_{(2)}^*$ is the effective permeability, is calculated in the second order of perturbation theory. It can be seen that for $\sigma_y^2 < 0.1$ $k_{(2)}^*$ and k^* are almost the same. Increasing σ_y leads to the rise of the difference between k^* and $k_{(2)}^*$.

Interference test Interference test involves more than one well. It is based on the analysis of pressure response in an observation well with respect to the rate in active well. Observation and active wells are remote by the distance $\Delta \mathbf{r}$. This distance $\Delta \mathbf{r}$ is usually larger compared with the permeability correlation length $\Delta \mathbf{r} > \lambda$. Pressure logarithmic derivative against time for this case is shown on Fig. 5. It can be seen that only the second plateau can be identified for the case $\Delta \mathbf{r} > \lambda$. For higher values of permeability correlation length $\Delta \mathbf{r} < \lambda$, its early-time behavior depends on λ .

Within the linear approximation with respect to σ_y^2 , it is possible to obtain analytical expression for the case of large times and $\Delta \mathbf{r} \gg \lambda$

$$\langle \delta p(\mathbf{r}, t) \rangle = -\sigma_y^2 \frac{pD}{4} \ln \left(\frac{\Delta \mathbf{r}^2}{4\bar{k}t} \right). \quad (25)$$

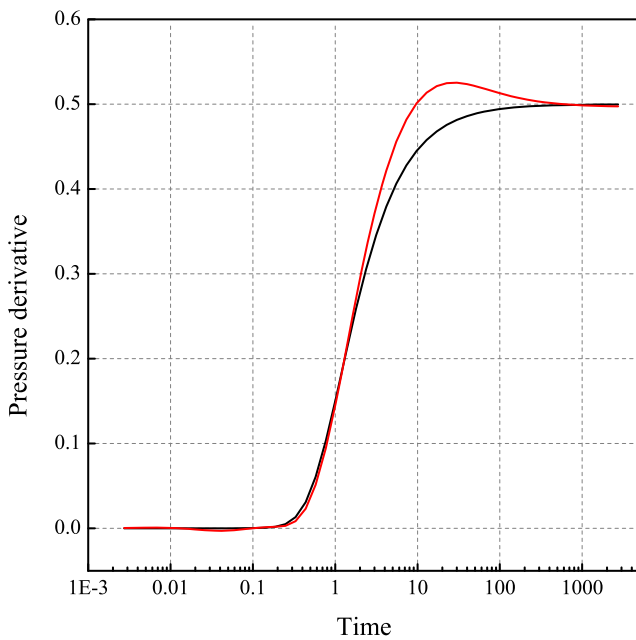


Fig. 5 Interference test. Logarithmic pressure derivatives for different values of correlation length $\Delta r = 100$ m and $\sigma_y^2 = 0.3$. Derivatives are normalized to geometric mean permeability whereas time is normalized to scale $\lambda^2/\langle\kappa\rangle$ with $\lambda = 50$ m. The black and red curves correspond to $\lambda = 50$ m and $\lambda = 500$ m respectively

From the comparison of (21) and (25), it can be seen that the effective reservoir permeability does not depend on relation between correlation length and the distance to observation point.

Pressure build-up test It is the most familiar well test. In this test, the well is shut off after a period of flowing at a constant rate, and the well pressure is recorded after shut-off. Laplace transform of well rate is given by

$$q_s = \frac{q_0}{s} - \frac{q_0 e^{-sT}}{s(1+s\tau)},$$

where τ is a characteristic time of wellbore storage effect, and T is a production time at constant rate q_0 before shut-off. Substitution of q_s in (18) leads us to the cumbersome expression for pressure distribution. However, pressure derivative can be represented by relatively compact expression

$$\frac{\partial \langle p \rangle}{\partial \ln(t)} = p_D \frac{t}{t_D} \int_0^\infty d\eta \eta J_0 \left(\eta \frac{\Delta r}{\lambda} \right) \left[\frac{-\frac{t+T}{t_D} \Phi(\sigma_y^2, \eta) \eta^2}{e^{-\frac{t+T}{t_D} \Phi(\sigma_y^2, \eta) \eta^2} - e^{-t/\tau}} - \frac{e^{-t/t_D} \Phi(\sigma_y^2, \eta) \eta^2}{t/t_D \Phi(\sigma_y^2, \eta) \eta^2 - 1} \right] \quad (26)$$

Figure 6 illustrates a number of pressure derivatives calculated for different values of variance σ_y^2 . Similar to other test types, these curves demonstrate two stabilization periods. Increase in variance leads to the fall of the second plateau which corresponds to greater effective permeability.

4 Applicability of the statistical approach

In this study, we consider pressure distribution averaged over ensemble of permeability realizations. However, in practice, we are dealing with a particular realization. Therefore, it should be understood when the spatial and ensemble averaging are the same. In other words, this approach is applicable if the specific “spatial” ergodicity or the “self-averaging” is observed. Since a porous media is statistically homogeneous, the spatial mean $\langle p_c \rangle$ can be defined as

$$\langle p_c(r) \rangle = \frac{1}{2\pi r} \int_L p(l) dl, \quad (27)$$

where the integration is carried out along the circle of radius r around a well. Here, we want to emphasize that the calculations are performed for a given permeability realization. The spatial mean $\langle p_c(r) \rangle$ should be compared

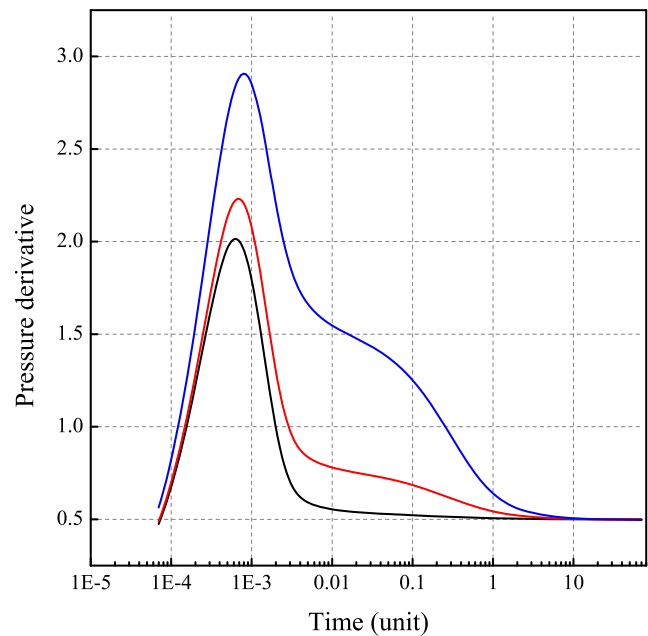


Fig. 6 Pressure derivative response in build-up well test for different variances of random permeability field with correlation length $\lambda = 300$ m. Derivatives are normalized to geometric mean permeability whereas time is normalized to $t_D = \lambda^2/\langle\kappa\rangle$, where $\langle\kappa\rangle$ corresponds to $\sigma_y^2 = 0.1$. The black, red, and blue curves correspond to $\sigma_y^2 = 0.1, 0.5, 1$ respectively. The dimensionless characteristic time of wellbore storage effect is equal to $\tau/t_D = 4 \times 10^{-3}$

Table 1 Parameters of the model

Drainage area	10000 x 10000 m ²
Thickness	10 m
Mean value	50 mD
Variance	15 mD
$\Delta x, \Delta y$	25 m
Δz	10 m
Well radius	0.1 m
Correlation length	900 m

with the stochastic mean $\langle p_s(r) \rangle$ which is calculated by averaging over ensemble of realizations. Our calculation is based on the ensemble averaging of 100 runs of flow simulator for each permeability realization. Realizations were generated using Sequential Gaussian Simulation with given correlation length and variance. Calculations were performed for a synthetic box-shaped model whose basic parameters are listed in Table 1. We use SI units through the paper. The comparison is done for sufficiently long time periods $t_D \approx 1.5$.

Figure 7 shows the relative discrepancy between $\langle p_r(r) \rangle$ and $\langle p_s(r) \rangle$ for the different numbers of averaged realizations. According to the figure, this discrepancy is small for any distances around well in case of sufficiently large time $t_D > 1$.

In order to illustrate how the condition of self-averaging affects the well test response, we perform the numerical

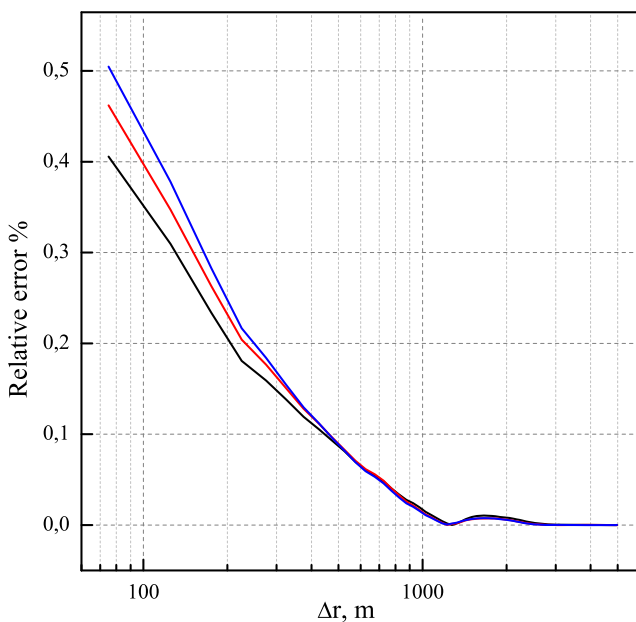


Fig. 7 Relative discrepancy between $\langle p_c \rangle$ and $\langle p_s \rangle$ against the distance from well. Red curve corresponds to discrepancy after 100 simulation runs. Black, blue curves correspond to 20 and 50 runs respectively

simulations of drawdown test using an industry reference reservoir simulator. Figure 8 shows the drawdown response data calculated for different realizations of a random permeability field. As it can be clearly seen, all curves in this figure have two stabilization periods. The second one is observed at sufficiently long times and it is almost the same for all permeability realizations. It means that the statistical approach is applicable for $t > t_D$. However, the initial stabilization period depends on a particular realization of permeability field and it is characterized by the permeability of the near wellbore zone.

The presence of two stabilization periods makes it possible to estimate the correlation length of the random permeability field. The initial pressure stabilization period can be used to determine the permeability in the bottomhole zone k_w , which isn't equal to k_H . This can be done using the expression (1). The correlation length of the permeability field can be estimated using the condition

$$\frac{\kappa_w t^*}{\lambda^2} = 1,$$

where t^* is determined from the time dependence of the pressure derivative and it approximately corresponds to the middle of the transition period. The shape of ramp depends on the type of semivariogram and it was numerically investigated in [9].

The level of the second stabilization period is associated with the effective permeability k^* . According to the expression (24), the effective permeability is complex

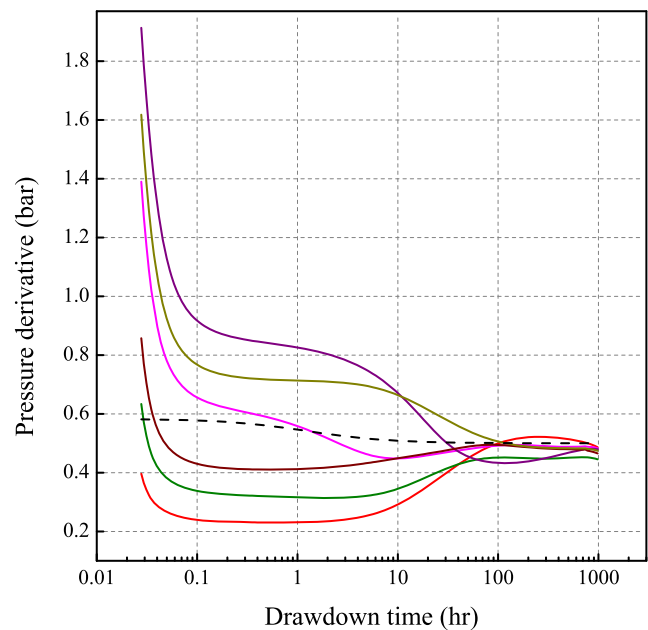


Fig. 8 Pressure logarithmic derivatives are calculated for several realizations of the random permeability field. Dashed line denotes to the mean derivative calculated according to the presented technique

parameter and it depends on both the mean value $\langle k \rangle$ and the variance σ_y^2 . The knowledge of the effective permeability does not allow us to determine σ_y^2 .

The dashed line in Fig. 8 indicates the level which corresponds to the effective permeability, which is given by (24). As it can be seen from this figure, simulation results are in a good agreement with results of this study.

In conclusion, we present some numerical estimations. Permeability correlation length varies from tens to several hundred meters. In the case of $k = 20(mD)$, $\mu = 1(cP)$ and $mc_t = 2 \times 10^{-10} (Pa^{-1})$ $\kappa = 0.1(m^2/s)$. Thus, for $\lambda = 100(m)$ the second stabilization period will be observed after 1.5 days. It means that well test duration should be sufficiently long.

Figure 9 demonstrates mean wellbore pressure and mean wellbore pressure logarithmic derivative calculated by industry reference simulator and according to the presented technique for $\sigma_y^2 = 0.25$. Both results practically coincides not only for late times $t/t_D \gg 1$, but even for $t/t_D < 1$ times. Initial deviation between curves is so-called pseudo wellbore storage effect coming from the use of stationary Peaceman equation in flow simulation.

Experimental observation of two stabilization periods on the pressure build-up curve was discussed in [14] and the results of the real extended test were presented. The well test data indicated a reduction of lateral permeability of

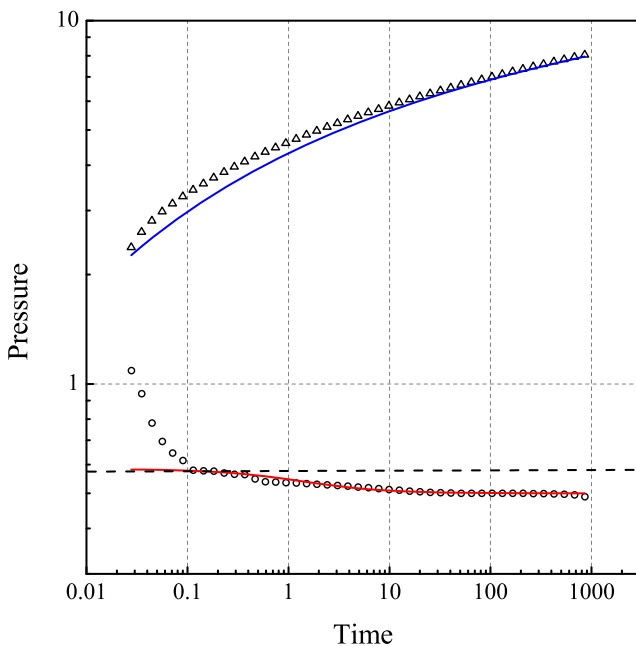


Fig. 9 Comparison of mean wellbore pressure and its logarithmic derivative calculated by industry reference simulator (triangles and circles) and according to the presented technique (blue and red solid lines) for $\sigma_y^2 = 0.25$. Derivatives are normalized to geometric mean permeability. Dashed line denotes to the early time plateau

formation. Such behavior is qualitatively consistent with the results of this work.

As we mentioned above, the results of this study were obtained under the assumptions of stationarity. However, stochastic approach can be used for the case of non-stationary permeability field and allows to consider conditioned realization. It can be done using perturbation-based moment equation approach [4], but it is almost impossible to solve the problem analytically. In this article, we focus on semi-analytical approach without engagement of serious numerical methods.

5 Conclusion

In this paper, we have considered the problem of transient flow in infinite stochastic porous media. The ensemble averaged pressure was found by solving the diffusivity equation where permeability was treated as a random field. The solution of a partial differential equation with stochastic coefficient is presented as a perturbation series in the permeability variance. The Feynman diagrams technique was used to calculate this series taking into account higher order terms. In the case of small permeability fluctuation, we have provided an analytical solution with respect to the second-order term in perturbation. The solution for ensemble averaged pressure was used to examine the effective permeability of porous media. The proposed analytical technique requires the stationarity of random permeability field. In the case of non-stationary permeability, field perturbation analysis can be done numerically [4]. Two practically important cases were considered. The first one corresponds to the situation when the distance Δr between a well and an observation point is much less than the correlation length λ . This is commonly true for drawdown or pressure build up tests. The second case corresponds to $\lambda \ll \Delta r$ which takes place in well interference test. We have proposed simple method to evaluate unknown geostatistical parameters such as the permeability variance and correlation length using pressure transient well test analysis. We have provided expressions that can be used to interpret various well tests.

Using numerical simulations, we have demonstrated that the discrepancy between the spatial and stochastic averaging is rather small and specific ergodicity is observed. This fact allows the stochastic approach to be applied to well test analysis for sufficiently long times.

Acknowledgments Authors would like to thank A. Ya. Shulman for helpful discussions on this work.

Appendix: Summation of perturbation series and Feynman diagrams technique

Here we formulate the Feynman rules for the calculation of the ensemble-averaged Green’s function of the diffusivity equation.

1. Bold line represents the Green’s function $G(\mathbf{p}, \mathbf{q})$
2. Solid line of momentum \mathbf{p} associates the factor $G_0(\mathbf{p})$
3. Dashed line of moment \mathbf{q} associates the factor $\tilde{\kappa}(\mathbf{q})$. It represents “interaction” with heterogeneities in porous media.

Under these rules the perturbation series (9) can be symbolized diagrammatically Fig. 10.

The ensemble averaged Green’s function is given by (10). The ensemble average is calculated by averaging over all realizations assuming appropriate statistical properties of the random permeability field. We suppose that permeability has log normal distribution and $\langle k \rangle$ is an arithmetic mean of lognormal distribution. If the variance is small compared with the mean value, a normal distribution approximation can be used to describe the permeability fluctuations. It is assumed that the permeability field is statistically homogeneous and the correlation function depends only on the distance between points $\rho_y = \rho_y(\mathbf{r} - \mathbf{r}')$. Applying Fourier transform yields

$$\langle \tilde{\kappa}(\mathbf{p}) \tilde{\kappa}(\mathbf{q}) \rangle = \langle \kappa \rangle^2 \sigma_y^2 \rho_y(\mathbf{p}) \delta(\mathbf{p} + \mathbf{q})$$

The averaging process can be illustrated diagrammatically by connecting all possible pairs of scatter lines. Each diagram can be referred to as irreducible or reducible. Figure 11 demonstrates the graphical representation of the expansion of the averaged Green’s function in a Gaussian random field. For any Gaussian field, there are only three irreducible diagrams and they are marked with numbers 1,3,4 in Fig. 11.

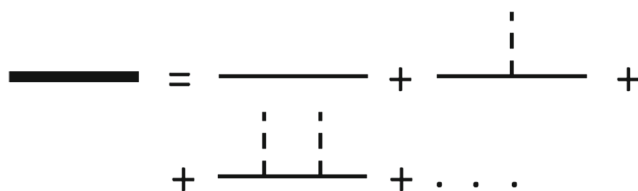


Fig. 10 Diagrammatic representation of perturbation series

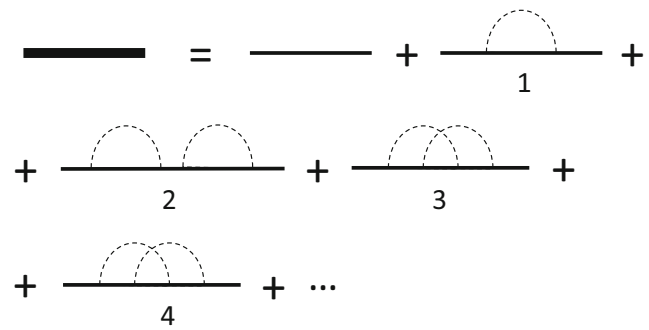


Fig. 11 Diagrammatic expansion of the averaged Green’s function in a Gaussian random field

For instance, the four points correlation function can be expressed as

$$\langle \tilde{\kappa}(\mathbf{p}) \tilde{\kappa}(\mathbf{q}) \tilde{\kappa}(\mathbf{p}') \tilde{\kappa}(\mathbf{q}') \rangle = \langle \tilde{\kappa}(\mathbf{p}) \tilde{\kappa}(\mathbf{q}) \rangle \langle \tilde{\kappa}(\mathbf{p}') \tilde{\kappa}(\mathbf{q}') \rangle + \langle \tilde{\kappa}(\mathbf{p}) \tilde{\kappa}(\mathbf{p}') \rangle \langle \tilde{\kappa}(\mathbf{q}) \tilde{\kappa}(\mathbf{q}') \rangle + \langle \tilde{\kappa}(\mathbf{p}) \tilde{\kappa}(\mathbf{q}) \rangle \langle \tilde{\kappa}(\mathbf{p}') \tilde{\kappa}(\mathbf{q}') \rangle.$$

The terms in the right side correspond to diagrams 2–4 correspondingly.

It is useful to define a self-energy function as the sum of all irreducible diagrams. In Fig. 12, the self-energy is shown with a crossed out circle and it is equal to the sum of three diagrams 1,3,4. Diagram 2 shown in the Fig. 11 is not included in self-energy because it is reducible and consists of two irreducible parts.

According to [2], diagrams 3 and 4 shown in Fig. 11 give small contribution to the self-energy compared to the diagram 1. Diagrams 3 and 4 contribute $1/\mathbf{p}$ compare with diagram of type 1; however, the correlation function is small for low values of \mathbf{p} .

A reasonable approximation for the self-energy in graphic form is presented in Fig. 13.

This diagram corresponds to explicit integral expression

$$\Sigma(\mathbf{p}) = G_0(\mathbf{p}) \int \mathbf{d}\mathbf{p}' G_0(\mathbf{p}') (\mathbf{p} \cdot \mathbf{p}') (\mathbf{p}' \cdot \mathbf{p}) C(\mathbf{p} - \mathbf{p}'),$$

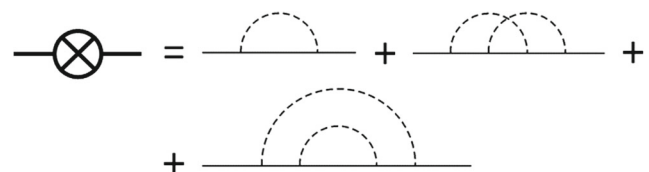


Fig. 12 Graphical representation for the self-energy

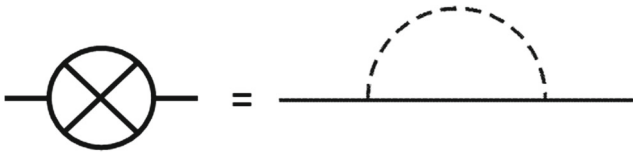


Fig. 13 Graphical representation of approximation for self-energy

where $C(\mathbf{p} - \mathbf{p}')$ is Fourier transform of the permeability covariance function. The Green’s function is expressed in terms of the self-energy part Σ as follows

$$\langle G(\mathbf{p}) \rangle = \frac{G_0(\mathbf{p})}{1 - G_0(\mathbf{p})\Sigma(\mathbf{p})}.$$

In the case of lognormal permeability field, three-point correlation terms are nonzero and should be taken into account. They make up σ_y^4 order contribution to the self-energy.

References

1. Svidler, M.I.: Statistical hydrodynamic of porous media. NEDRA, Moscow, 689 (1985)
2. King, P.R.: The use of field theoretic methods for the study of flow in a heterogeneous porous medium. *J. Phys. A: Math. Gen.* **20**, 3935–3947 (1987)
3. Zhang, D.: Numerical solution to statistical moment equations of groundwater flow in nonstationary, bounded, heterogeneous media. *Water Resour. Res.* **34**(3), 529–538 (1998)
4. Li, L., Tchelepi, H.A., Zhang, D.: Perturbation-based moment equation approach for flow in heterogeneous porous media:

- applicability range and analysis of high-order terms. *J. Comput. Phys.* **188**(1), 296–317 (2003)
5. Jarman, K.D., Russel, T.F.: Eulerian moment equations for 2-D stochastic immiscible flow. *Multiscale Model Simul.* **1**(4), 598–608 (2003)
6. Tartakovsky, D.M., Neuman, S.P.: Transient effective hydraulic conductivity under slowly and rapidly varying mean gradients in bounded three-dimensional random domain. *Water Resour. Res.* **34**(1), 21–32 (1998)
7. Sanchez-Vila, X., Tartakovsky, D.M.: Ergodicity of pumping tests. *Water Resour. Res.* **43**, W03414 (2007)
8. Netinger, B., Gautier, Y.: Use of the Fourier-Laplace transform and of diagrammatical methods to interpret pumping tests in heterogeneous reservoirs. *Adv. Water Resour.* **21**, 581–590 (1998)
9. Hamdi, H.: Well-test response in stochastic permeable media. *J. Pet. Sci. Eng.* **119**, 169–184 (2014)
10. Edwards, S.F.: A new method for the evaluation of electric conductivity in metals *Phil.Mag.* 3, 33, p. 1020–1031 (1958)
11. Morse, P.M., Feshbach, H.: *Methods of Theoretical Physics Part I*. New York: McGraw-Hill, pp. 501–502, 513–514 and 656, 1953
12. Neuman, S.P., Orr, S.: Prediction of steady state flow in nonuniform geologic media by conditional moments: exact nonlocal formalism, effective conductivities, and weak approximation. *Water Resour. Res.* **29**(2), 341–364 (1993)
13. Dagan, G.: Analysis of flow through heterogeneous random aquifers, 2. Unsteady flow in confined formations. *Water. Resour. Res.* **18**, 1571–1585 (1982)
14. Hamdi, H., Rueland, P.: Using geological well testing for improving the selection of appropriate reservoir models *Petroleum Geoscience* (2014)

Publisher’s note Springer Nature remains neutral with regard to jurisdictional claims in published maps and institutional affiliations.

Affiliations

A. V. Novikov¹ · D. V. Posvyanskii²

A. V. Novikov
Aleksei.Novikov@Emerson.com

¹ Roxar AS, Moscow, Russia
² Institute of Radio-engineering and Electronics RAS, Moscow, Russia